

# Designing Stimulation Patterns for an Afferent BMI: Representation of Kinetics in Somatosensory Cortex

Brian M. London, *Student Member, IEEE*, Ricardo Ruiz Torres, Marc W. Slutzky, *Senior Member, IEEE*, and Lee E. Miller, *Member, IEEE*

**Abstract**—In recent years, much attention has been focused on developing stimulating strategies for somatosensory prostheses. One application of such a somatosensory prosthesis is to supply proprioceptive feedback in a brain machine interface application. One strategy for the development of such a stimulation regime is to mimic the natural representation of limb state variables. In this paper, we demonstrate that end point force is represented in primary somatosensory cortex of the macaque and force, in addition to velocity, can be decoded from S1 neural recordings. Force is represented in S1 in both a movement and isometric tasks; however, models that predict force in one condition do not generalize to the other. Possible interpretations of these apparently contradictory results are discussed.

## I. INTRODUCTION

RECENT years have seen an increasing interest in developing a somatosensory afferent brain machine interface (BMI) [1, 2]. To supplement a motor BMI, proprioceptive or tactile feedback would be supplied to the user through electrical stimulation in the brain, spinal cord, or peripheral nerves. The ability to make normal movements is severely impaired in patients who lose proprioception despite intact motor and visual systems [3]. Visual feedback alone is insufficient for normal motor function.

One potential location for stimulation to evoke an artificial sensation of proprioception is primary somatosensory cortex (S1). It has been shown that electrical stimulation of proprioceptive regions in S1 can evoke conscious perceptions [4]. Moreover, information conveyed by electrical stimulation in S1 can be used by a monkey performing a BMI task [2].

Designing a stimulation paradigm to convey meaningful proprioceptive information is a daunting task. The potential space of all stimulus trains is enormous for even a single electrode and grows geometrically for each additional electrode. Stimulators with upwards of 1000 electrodes are

under development [5] and the number of channels are growing constantly.

One way to reduce the stimulus feature space that must be explored is to limit stimulation patterns to the space of natural activity patterns encoding limb state in the intact animal. That is, determine the normal representation of proprioception in S1 and design stimuli that mimic it. For cutaneous input there is evidence that biomimetic stimulation mimicking the discharge patterns evoked by natural afferent inputs evokes perceptions that are similar to those of the natural inputs [6].

In this study we investigate the extent to which force, in addition to kinematics, is represented in S1. Whether cortical representations of proprioception include kinetic as well as kinematic variables is an important question not only for designing BMIs but also for understanding the sensory-motor system of the brain as a control system for movement.

## II. METHODS AND ANALYSIS

### A. Behavioral Paradigms

Two monkeys (T and M) were each trained on two different behavioral paradigms. In all cases the monkey sat in a primate chair facing a video screen and grasped a handle that was placed in front of them. The handle was attached to a six-axis force/torque sensor (nano-30; ATI Automation). In the movement paradigm, the handle was attached to the end of a two link planar manipulandum. Targets were presented on the video screen along with a cursor that tracked the position of the handle. The monkey was required to move the cursor into the target. Targets were uniformly distributed over the 30 cm×30 cm workspace. Upon hitting several targets in a row the monkey would receive a liquid reward.

Motors attached to the manipulandum were used to apply background force loads (loaded movement paradigm). This background force was configured to drift chaotically and slowly in magnitude and direction during the task such that over the course of several minutes interaction force between the monkey hand and the handle was effectively decorrelated from the movement of the handle.

In the isometric paradigm, the handle was rigidly positioned in front of the monkey. The cursor position was mapped to the forces exerted on the handle in the horizontal plane. Again, targets were randomly positioned and the monkey needed to move the cursor into the targets in a sequence that imitated that of the movement paradigm.

Manuscript received April 15, 2011. This work was supported by the National Institutes of Health under Grant NINDS NS048845.

B. M. London is with the Northwestern University Interdepartmental Neuroscience Program, Chicago, IL 60611 USA (e-mail: blondon@u.northwestern.edu).

R. Ruiz Torres, is with the Northwestern University Interdepartmental Neuroscience Program, Chicago, IL 60611 USA.

M. W. Slutzky is with the Departments of Neurology, Physical Medicine and Rehabilitation, and Physiology, Feinberg School of Medicine, Northwestern University, Chicago, IL 60611 USA.

L. E. Miller is with the Departments of Physiology and Physical Medicine and Rehabilitation, Feinberg School of Medicine, and the Department of Biomedical Engineering, Northwestern University, Chicago, IL 60611 USA (phone: 312-503-0752 e-mail: lm@northwestern.edu).

Example force and velocity trajectories are shown in Fig. 1.

### B. Neural Recordings

We surgically implanted 96-electrode silicon arrays (Blackrock Microsystems) in the post-central gyrus of the monkeys under isoflurane and remifentanyl anesthesia. The location was chosen through intra-operative surface recordings to include proprioceptive proximal arm representation. Histological results from a monkey with a similar implant (not presented here) suggest that the arrays were predominantly in Area 2 with a few electrodes in Area 1. After surgery, monkeys were provided buprenorphine analgesic and given a week to recover before returning to the behavioral task. Sensory field mappings indicated that both arrays were in the proximal arm region and had neurons with a mixture of proprioceptive and cutaneous receptive fields. All procedures were conducted in accordance with the National Research Council Guide for the Care and Use of Laboratory Animals and a protocol approved by the Northwestern University Institutional Animal Care and Use Committee.

Neural data, force measurements, and (where applicable) handle position were collected using a neural data acquisition system (MAP; Plexon). All comparisons made across behavioral paradigms were made from data collected in single sessions. Neurons were discriminated offline using Offline Sorter (Plexon) and only those neurons that showed stable isolation through all behavioral paradigms were included for analysis.

### C. Data Analysis

Data were imported into MATLAB (Mathworks) for analysis. Firing rate modulation depth was calculated for each neuron for each task. We binned the spike data into 0.5 second blocks and took the average of the five highest and five lowest firing rate blocks. The difference between these two averages was defined as the depth of modulation.

Predictions of force and velocity were made using a Wiener filter as described elsewhere [7]. Briefly, the Wiener filter attempts to predict the force or kinematic signal as a linear combination of binned firing rates from each neuron over several lags. Neural data were binned and force and velocity were discretized at 25 ms. The Wiener filter was fit using ten lags symmetrically spanning zero, since unlike motor cortical neurons, most of the modulation of these cells is due to afferent input that lags movement. The lags were selected because they span the range over which these cells were most informative about kinematics.

All predictions shown were 10-fold cross-validated. Where goodness of fit measures are presented they are shown as mean  $\pm$  standard deviation across folds. Axes were defined in the horizontal plane with X being positive to the monkey's right and Y being positive away from the body of the monkey.

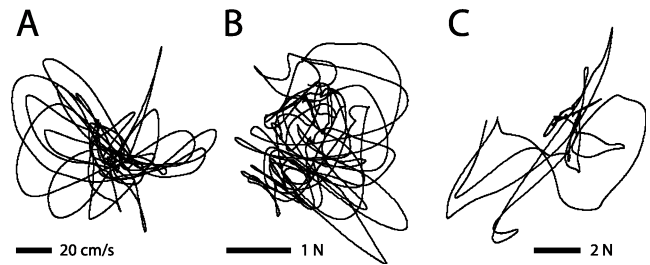


Fig. 1. Traces from representative 15 second segments of the movement task (A and B) and the isometric task (C). Paths shown depict handle velocity (A) and force (B and C). Both the movement and isometric tasks caused decorrelated X and Y forces although the isometric task force changes were slower and had larger excursions (note different scale in (C))

## III. RESULTS

### A. Modulation to Movement and Isometric Forces

We collected data from both monkeys during the loaded movement and isometric tasks and from monkey T in the unloaded movement condition. Recordings contained 37 units for monkey M and 30 units for monkey T. Example force and velocity traces are depicted in Figure 1. For each panel, the path through force or velocity space was traced for 15 seconds. Panel A shows velocity during the movement task and B shows force during the movement task. The lower density of trajectories in the isometric task (C) reflected the less frequent movements made by the monkey. However peak force was higher in the isometric case than in the movement task (Note: different scales).

Neurons recorded from both monkeys responded robustly to all behavioral paradigms. It was not the case that particular neurons were responsive to one or the other behavioral paradigm. Instead, neurons that responded in the

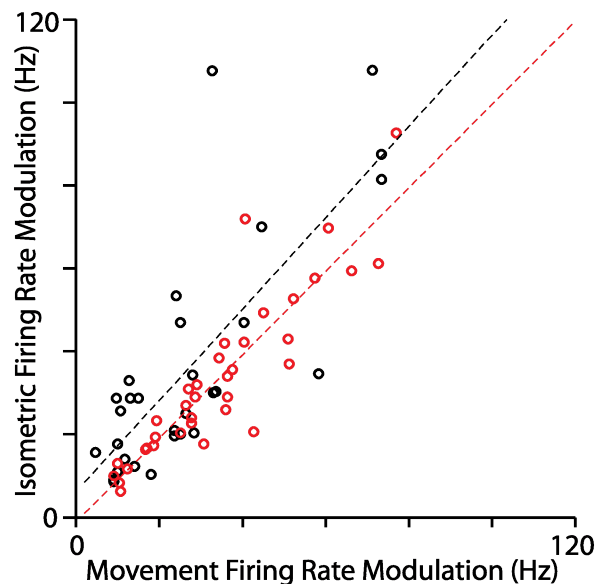


Fig. 2. Depth of modulation of individual neurons from monkeys T (black) and M (red) for the loaded movement task and the isometric task. Responses of individual cells tended to be highly correlated across the two conditions.

movement condition tended also to respond in the isometric task. The responses to the loaded movement and isometric task are plotted in Figure 2. The modulation depths in the two tasks were highly correlated with slopes near 1. (Monkey M: slope=1.0  $R^2=0.80$   $p<10^{-12}$ , Monkey T: slope=1.1  $R^2=0.60$   $p<10^{-6}$ ) There was a slight tendency for monkey T's neurons to modulate more in the isometric task.

### B. Predictions of Force and Velocity

We were able to predict velocity accurately in both the loaded and unloaded conditions and were able to predict force in the unloaded and isometric conditions but not the loaded movement condition. Example traces of actual force

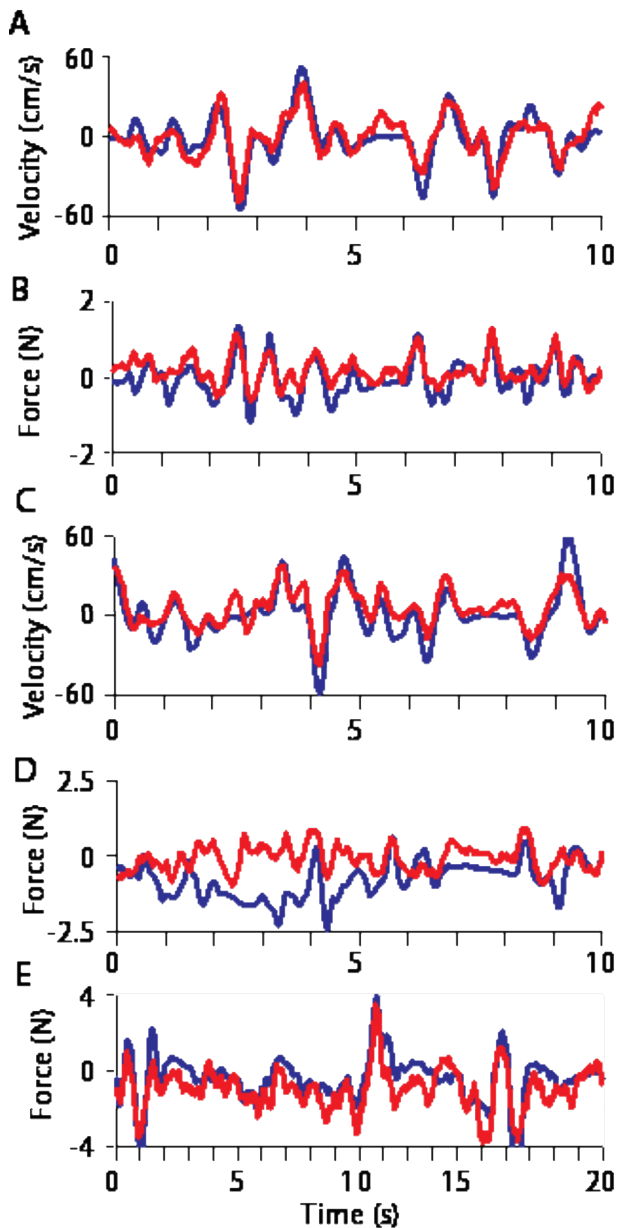


Fig. 3. Actual (blue) and predicted (red) velocity and force for the three tasks. Shown are the unloaded paradigm velocity (A) and force (B), loaded velocity (C) and force (D), and force in the isometric task (E). The pairs of panels A-B and C-D each represent force and velocity recorded simultaneously.

or velocity and the corresponding predictions are depicted in Figure 3. In all cases the X component of the force or velocity is depicted. Y components of the predictions were similar (See: below and Figure 4).

Velocity predictions tended to be good in both the loaded and unloaded movement paradigms (Figure 3 A and C). In the unloaded case, force was also predicted well (B). As can be seen, the force in the unloaded condition resembles the derivative of the velocity. In the loaded condition, however, the slow drift of force due to the loads is obvious (D). The linear model was unable to capture this perturbation. In the isometric task, the model was again able to predict force accurately (E). The time axis is different in panel E as a consequence of the lower rate of reaches described above. This ability to predict force during the isometric condition suggests that any correlations between force and velocity are not sufficient to explain the force predictions in the unloaded case, since the hand velocity was zero throughout the isometric block.

These prediction results were consistent for movements and forces in both the X and Y directions and between monkeys. Figure 4 shows the mean coefficients of determination of predictions with standard deviation across folds. In the unloaded condition, the model performed well, with a level of performance similar to what we have observed in other monkeys in this task [8]. In the loaded condition the quality of the predictions persisted, with an  $R^2$  around 0.65. The force predictions in the unloaded and isometric cases were reasonably good as well ( $R^2$  around 0.5), although not as good as the velocity predictions. Force predictions across directions and monkeys were consistently

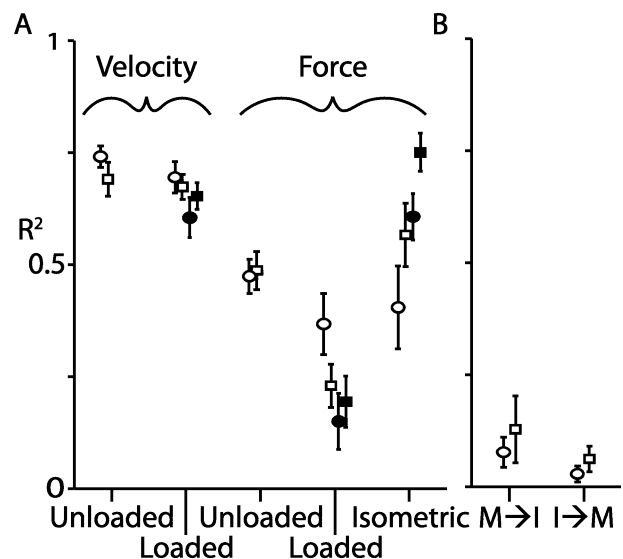


Fig. 4. Goodness of fit measures for 10-fold cross validated predictions of velocity and force within conditions (A) and across conditions (B). Glyphs and error bars indicate mean and standard deviation across folds.  $R^2$  values of predictions from X (circle) and Y (square) directions and Monkeys T (empty) and M (filled) are depicted. We were able to predict velocity accurately with and without loads and force in the isometric and unloaded conditions but not in the loaded condition. The force models did not generalize across conditions.

poor for the loaded movement task.

### C. Generalization of Models

The models that accurately predicted force from neural activity in the unloaded and isometric conditions did not generalize across tasks. The coefficients of determination plotted in Figure 4B show the results when the model was trained on one condition and testing on the other. These are the same filters used for Monkey T force predictions in the isometric and unloaded columns of panel A, but tested on the opposite conditions. This lack of generality demonstrates that while we are able to decode force in both conditions, the neural representation of force in these conditions appears not to be the same.

## IV. DISCUSSION

Any afferent BMI using S1 stimulation to supply proprioceptive feedback will have to include force information, for which vision is even more ill-suited than for kinematics. The ability to convey force, in addition to kinematic information, is potentially useful as well since so many activities of daily living involve movements that encounter resistance. We have demonstrated the ability to decode force from S1 neurons in an isometric task. Because this task involved no movement of the limb, the ability to decode force cannot be due to correlations of force with kinematic variables of the limb itself. This suggests that in addition to kinematic variables, kinetics of the limb are represented in S1. We have identified area 2 as a potential location to stimulate for force feedback in a BMI application.

Somewhat surprisingly, the amount of modulation of individual neurons was similar across the isometric and movement tasks. In earlier work, we and others have demonstrated that neurons in area 2 encode position and velocity in varied proportion. Likewise, different cells respond to greater or lesser extent to active and passive limb movement [8, 9]. In contrast, there was not such a continuous distribution between cells that responded to velocity, force, or a combination of the two variables. Rather, neurons responded to both or neither. This suggests that area 2 naturally encodes a mixture of force and velocity – perhaps some latent variable that represents both. Possibilities for this latent variable include muscle forces or the time derivative of endpoint force. Determining exactly what this latent variable is should be a goal of future study.

In considering why our models failed to generalize, it is important to note that the force we measured is the interaction force between the handle and the monkey's hand. In the movement task this may be quite different from forces actually exerted by the muscles (and sensed by Golgi tendon organs) since forces exerted to accelerate the mass of the limb would not be measured at the handle. However, in the isometric task, handle and muscle forces would be highly correlated since the movement dynamics are eliminated. Perhaps, a model fitting a latent variable as described above

would be able to generalize or fit the loaded force condition. For example, if the neurons really encode muscle force, then they should be predictive of endpoint force in the unloaded movement task since most of the measured force goes to accelerating the inertial load of the arm and robot, which would be correlated. However, in the loaded task this correlation would be broken by the loads, thus making muscle force no longer predictive of endpoint force.

The models used in this study were all linear. There may be a non-linear model that would represent a mixture of velocity and force consistently across our varied experimental paradigms. It is also possible that our failure to find a single linear model that spanned this space was a limitation primarily of our model identification methods rather than the linearity of the system. Since the movement and isometric tasks each have combinations of force and velocity not present in the other task, a better test may be to train a linear decoder on a more robust training set that spans the full range of both paradigms. This would eliminate the need for the model to extrapolate to force/velocity combinations on which it was not trained.

As a future endeavor, we intend to pursue the question of the independent representation of the kinetics and kinematics of active and passive movement. Our results suggest that force, in addition to kinematics, will be an important component of those stimulation efforts.

## V. REFERENCES

- [1] R. A. Gaunt, J. A. Hokanson, and D. J. Weber, "Microstimulation of primary afferent neurons in the L7 dorsal root ganglia using multielectrode arrays in anesthetized cats: thresholds and recruitment properties," *J. Neural Eng.*, vol. 6, p. 055009, 2009.
- [2] J. E. O'Doherty, M. Lebedev, T. L. Hanson, N. Fitzsimmons, and M. A. L. Nicolelis, "A brain-machine interface instructed by direct intracortical microstimulation," *Front. Integr. Neurosci.*, vol. 3, 2009-September-1 2009.
- [3] J. Gordon, M. F. Ghilardi, and C. Ghez, "Impairments of reaching movements in patients without proprioception. I. Spatial errors," *J. Neurophysiol.*, vol. 73, pp. 347-360, January 1, 1995.
- [4] B. M. London, L. R. Jordan, C. R. Jackson, and L. E. Miller, "Electrical Stimulation of the Proprioceptive Cortex (Area 3a) Used to Instruct a Behaving Monkey," *IEEE Trans. Neural Sys. Rehab. Eng.*, vol. 15, p. In press, 2008.
- [5] A. M. Wilder, S. D. Hiatt, B. R. Dowden, N. A. T. Brown, R. A. Normann, and G. A. Clark, "Automated Stimulus-Response Mapping of High-Electrode-Count Neural Implants," *Neural Systems and Rehabilitation Engineering, IEEE Transactions on*, vol. 17, pp. 504-511, 2009.
- [6] R. Romo, A. Hernandez, A. Zainos, C. D. Brody, and L. Lemus, "Sensing without Touching: Psychophysical Performance Based on Cortical Microstimulation," *Neuron*, vol. 26, pp. 273-278, 2000.
- [7] A. H. Fagg, G. W. Ojakangas, L. E. Miller, and N. G. Hatsopoulos, "Kinetic Trajectory Decoding Using Motor Cortical Ensembles," *Neural Systems and Rehabilitation Engineering, IEEE Transactions on*, vol. 17, pp. 487-496, 2009.
- [8] B. M. London, R. R. Torres, and L. E. Miller, "Towards a bidirectional brain-machine interface: Coding properties of proprioceptive cells in somatosensory cortex," in *Society for Neuroscience San Diego*, 2010.
- [9] M. J. Prud'homme and J. F. Kalaska, "Proprioceptive activity in primate primary somatosensory cortex during active arm reaching movements," *J. Neurophysiol.*, vol. 72, pp. 2280-2301, November 1, 1994.